V European Conference on Computational Fluid Dynamics
ECCOMAS CFD 2010
J. C. F. Pereira and A. Sequeira (Eds)
Lisbon, Portugal,14-17 June 2010

AN IMMERSED BOUNDARY METHOD FOR LARGE-EDDY SIMULATION OF FULLY COMPRESSIBLE FLOWS: APPLICATION TO TRANSONIC CAVITY FLOW

C. Merlin*, P. Domingo*, L. Vervisch* and G. Lodato†

*CORIA-CNRS and INSA de Rouen, Campus de Madrillet
Avenue de l'Université, BP 8, 76801 Saint Etienne du Rouvray Cedex, France
e-mail: cindy.merlin@coria.fr, pascale.domingo@coria.fr and luc.vervisch@coria.fr
†Present address: Center for Turbulence Research
Stanford, California, USA

Key words: Immersed Boundary Method, Boundary Conditions, Large Eddy Simulations, Navier Stokes Characteristic Boundary Conditions

Abstract. *The application of the Immersed Boundary Method (IBM) for performing Large-Eddy Simulation (LES) of viscous, turbulent and compressible flows around various complex configurations is presented. Turbulence is addressed by LES using a fourth order numerical scheme with various Sub-Grid Scale (SGS) models: the MiLES approach, the Vreman model, the lagrangian dynamic Smagorinsky closure and the localized dynamic version. A methodology to compute the SGS terms near immersed boundaries is also discussed. A transonic cavity flow is then studied. This flow is known to exhibit self-sustained oscillations generated by a flow-acoustic resonance mechanism. The quality of the immersed boundary method is evaluated against auxiliary computations based on a cartesian multi-block grid mesh without wall reconstruction and with characteristic boundary conditions. This study illustrates the ability of the immersed boundary concept to deal with compressible flows.*

1 INTRODUCTION

The Trapped Vortex Combustor (TVC) is a challenging configuration providing high combustion efficiency, low emission and low pressure drop. The flow is trapped within a cavity where the reactants are mixed. Flame stabilization is achieved through the recirculation zones induced by the cavity with a trapped turbulent vortex. Some experimental and numerical studies have been devoted to the effective use of cavities to suppress combustion instability [1,2,3,4]. Generally, a bluff body is located upstream to initiate shear layer instabilities, which are then trapped in the cavity region and provides a wake to help the flame stabilization.

The numerical study of a non rectangular configuration with a bluff body is possible in a non-structured solver. Another approach retained in this paper is to keep a structured mesh with the addition of an immersed boundary concept. Immersed Boundary Methods employ cartesian meshes that do not conform to the shape of the body in the flow and modify the governing equations to incorporate the boundary conditions. First introduced by Peskin [5], IBMs involve either continuous or discrete forcing approaches. Only discrete forcing approach preserves good performance at high Reynolds number. The ghost-cell method (discrete forcing approach) utilizes a sharp boundary with a modification of the computational stencil and an extrapolation scheme to deduce the state variables in the border cells.

To evaluate the accuracy of the boundary layers reconstruction with an immersed boundary, a transonic cavity configuration without combustion is simulated for which measurements are available in the literature. Such high velocity subsonic flow exhibits strong aeroacoustic oscillations due to a coupling between pressure disturbances and the vortical structures. This feedback loop is generated by the impact of the shear layer on the downstream wall leading to the subsequent generation of acoustic waves which initiates further instabilities. Numerous experimental studies have been devoted to the study of such an aeroacoustic loop with the pressure spectrum (radiation acoustic analysis). However, only a few of them have investigated the velocity field inside the cavity. A complete data set concerning the flow features is available in the experiment of Forestier *et al.* [6,7] Concerning the numerical investigations, many LES computations have been performed to characterize the acoustic radiation of cavities [8,9]. The major results are obtained at transonic Mach number. An extensive analysis of the cavity flow fields have been provided by Larchevêque *et al.* [10,11,12] and Sagaut *et al.* [13]

In the following sections, the numerical method as well as the boundary conditions methodology are briefly described. The validation of the immersed boundary method is discussed with some test cases. The cavity flowfield is then investigated. Finally, the accuracy of the method is demonstrated by comparing the results obtained with the immersed boundary method and with a multi-block approach combining characteristic boundary conditions in the case of a pressure wave within a closed box, and, of the flow over a cavity.

2 GOVERNING EQUATIONS

The governing equations considered are the unsteady Navier-Stokes equations for a viscous compressible flow. In order to follow the flow field and essentially the shedding process, a passive scalar quantity Z is transported thus introducing an additional transport equation.

The solver is a parallel one based on an explicit finite volume scheme for cartesian grids. The convective terms are computed resorting to the fourth-order centered skew-symmetric-like scheme proposed by Ducros *et al.* [14] The diffusive terms are computed using a fourth-order centered scheme. In order to suppress spurious oscillations and damp high-frequency modes, the numerical scheme is augmented by a blend of second- and fourth-order artificial terms [15]. Time integration is performed using a third-order Runge-Kutta scheme [16]. To avoid the flow structures distortion, the boundaries are described using the three-dimensional Navier-Stokes characteristic boundary conditions approach to describe non-reflective boundary conditions [17]. This method is particularly effective in the context of compressible flows which prevent the appearance of spurious reflections at the open boundaries.

The immersed boundaries method has already been combined with high-order scheme in the DNS context by Lamballais and Silvestrini [18] and in compressible LES by De Palma *et al.* [19] The present approach employs a ghost-cell technique for imposing the boundary conditions on the immersed boundaries [20,21,22,23]. The interpolation scheme for the cells cut by the immersed boundary is based on the determination of an image-point expressed in terms of a linear, bi-linear or tri-linear interpolation. The boundary conditions are described by a Neumann condition for pressure ($\partial P/\partial n = 0$, where n is the direction normal to the immersed surface) and Dirichlet conditions for velocities (no-slip conditions). The wall temperature is calculated by using an adiabatic hypothesis.

Large-Eddy simulations have been carried out with various subgrid strategies. The first approach is an implicit one denoted MiLES [24]. The next ones rely on traditional SGS modeling approach: the Vreman model [25], the Lagrangian Dynamic Model indicated as LDSM [26] and the Localized Dynamic Smagorinsky Model [27]. The last one is based on a filtering operation which introduces the right amount of viscosity in the vicinity of walls. The test filter is described by a trapezoidal rule [28]. The filtered quantities near the immersed boundaries are determined by cutting the filtering volume. More precisely, the scheme is switched to bi-dimensional filtering over the plane parallel to the immersed boundary and ghost cells are not included in the filtering operation. In a similar manner, the lagrangian reconstruction of the fluid path in the LDSM is modified in the vicinity of the immersed and real boundaries.

Since the turbulent viscosity on the wall is zero, a new interpolation scheme is proposed. It relies on the Dirichlet condition for the turbulent viscosity to recover the correct ghost viscosity. To determine the SGS viscosity near the boundaries, a tri-linear interpolation scheme is thus used.

3 VALIDATION OF THE IBM SOLVER

To validate the numerics and the modeling, the wake behind an unconfined circular cylinder is first computed and results are compared with previous simulations and experiments. This preliminary test case is studied in a 2D DNS framework. The flow Reynolds number is $Re_d = 300$ with d the cylinder diameter. The results are compared against experimental and previous simulation [29,30]. Figure 1 shows the variation of the drag and lift coefficients. The mean drag and Strouhal numbers determined from these time evolutions are $C_D = 1.37$ and $St = 0.21$, which are the expected values [29,30].

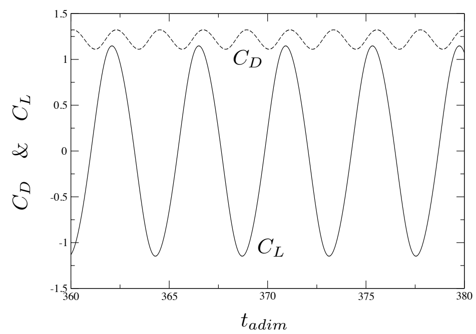

Figure 1: Variations of drag and lift coefficients with time of the flow past a circular cylinder with $Re_d = 300$.

The next test consists of a turbulent flow past a square cylinder. This cylinder has a rectangular cross-section of dimension d immersed in a uniform velocity stream. The Reynolds number based on the side dimension d is fixed to 22 000. This flow was investigated experimentally by Lyn *et al.* [31] and McLean *et al.* [32] The study is conducted with Large Eddy Simulation where subgrid viscosity is determined with the WALE model. Symmetry and periodic boundary conditions are applied respectively in the normal direction (y) and in the spanwise direction (z) corresponding to the cylinder's axis. Grid is refined around the cylinder to preserve a good accuracy in its vicinity. The adiabatic no-slip walls constituting the square are not coincident with the grid meshes. The open boundaries are non-reflecting ones with a uniform stream u_∞=1, and v=0 and w=0 for the inlet. To reproduce the free-stream turbulence level measured upstream of the cylinder [30], namely 2 percent with regard to the meanstream, a correlated random noise is superimposed to the average velocity profiles with the Klein turbulent injection [33]. The Fig. 2 compares streamwise and normal averaged velocities with experimental data on the cylinder and in its wake. A satisfactory agreement is observed.

4 LARGE EDDY SIMULATION OF A CAVITY FLOW

The structure of an unsteady flow past a rectangular open cavity is then investigated using cartesian grids with non conforming boundaries to discretize the governing equations.

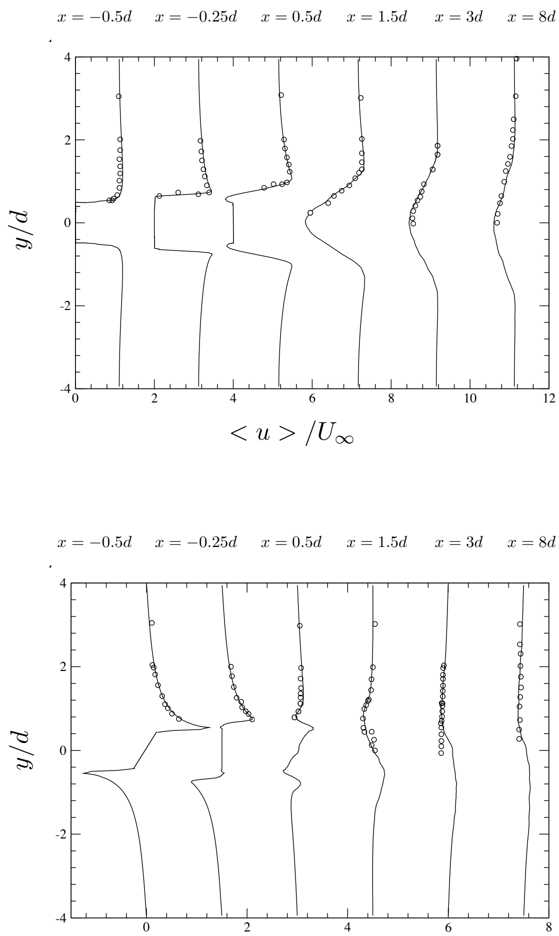

Figure 2: Time-averaged streamwise and normal velocity U and V at various locations expressed (lines) w.r.t. experimental data (dot).

The 3D cavity configuration studied is of parallelepiped shape and has a length-to-depth ratio of $L/D = 2$ and a depth ratio of $W/D = 4.8$. The dimensions of the computational domain are presented in Fig. 3. It was studied experimentally by Forestier *et al.* [6,7] The inflow Mach number is $M = 0.8$ while the Reynolds number is $Re_L = 6.8 \times 10^6$, based on the length of the cavity.

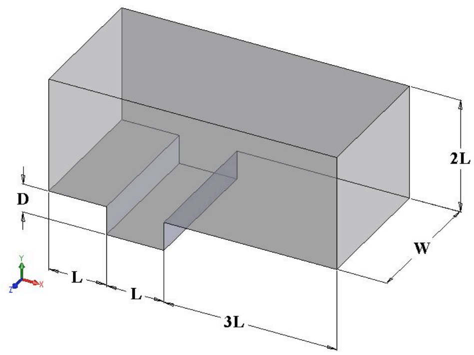

Figure 3: Dimensions of the computational domain for the cavity study.

To perform this immersed boundary study, the grid points are clustered near all the walls and in the shear layer above the cavity. The characteristics of the mesh are summed up in the table 4 with typical dimensions of the boundary layer in local wall units. The mesh contains 6.6 millions cells.

For flows with self-sustained oscillations, open boundaries have to be treated with great care. The previously mentioned 3D-NSCBC approach [17] has been used to avoid any spurious reflections. For the inflow conditions, fluctuations have been added to the main profile. This synthetic turbulence is space and time-filtered correlated using the digital filter approach of Klein *et al.* [33] Nevertheless, in this particular configuration, the turbulent injection does not play a crucial role in the self-sustained oscillations. The numerical simulations carried out in this study revealed that the turbulence is mainly generated by the Kelvin-Helmholtz instability and the recirculation zones. This result was already mentioned by Sagaut *et al.* [13] for the same configuration.

The study of Larchevêque *et al.* [12] employed MiLES and Selective Mixed Scale modeling

$Mesh$	$290 \times 188 \times 122$
Δx^+	$30 \sim 130$
Δy^+	$20 \sim 70$
Δz^+	$15 \sim 30$
Δt	$3.8 \times 10^{-7} s$

Figure 4: Mesh properties

strategies. In the present study, the LES investigation is expanded beyond the use of the MiLES approach by using the Localized Dynamic Smagorinsky and the Vreman models presented previously.

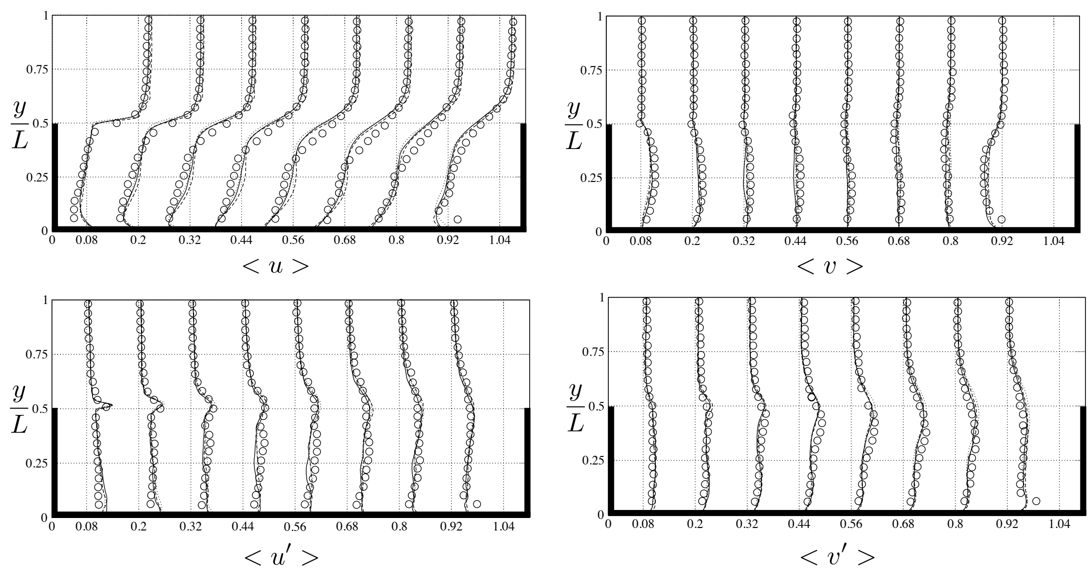

Figure 5: Velocity statistics in the mid-span plane with immersed boundaries: longitudinal mean velocity, vertical mean velocity, longitudinal fluctuating velocity and vertical fluctuating velocity: — LDSM, - - - MiLES, · · · Vreman model and ∘ experimental data.

The Fig. 5 shows that the simulations accurately reproduce the first and second order statistics. All the SGS strategies accurately describe the statistical properties of the flow.

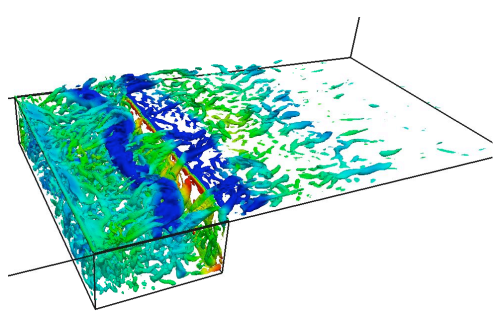

Figure 6: Three-dimensional vortical structures defined by the Q criterion with the Localized Dynamic Smagorinsky Model for the subsonic cavity.

The key feature of the cavity flow is the presence of specific turbulent structures well described with the simulations. Figure 6 shows the 3D views of the Q-criterion using our approach with immersed boundaries. The interactions of coherent structures with the downstream edge are predominant due to flow impingement and recirculation.

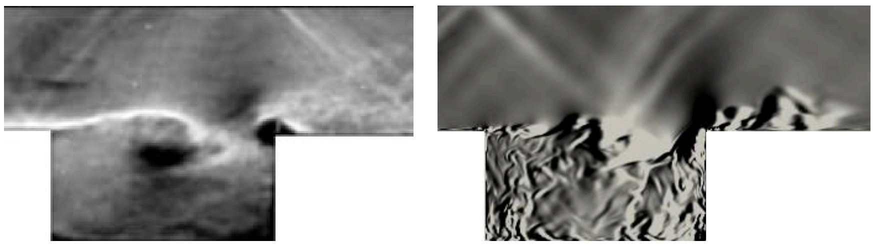

Figure 7: An experimental fast Schlieren view (left)[7] and a strioscopic view from the MiLES computation (right).

The Fig. 7 presents a comparison between an experimental fast Schlieren view of Forestier *et al.* [7] and a numerical strioscopic view at a similar time. The waves pattern is well recovered.

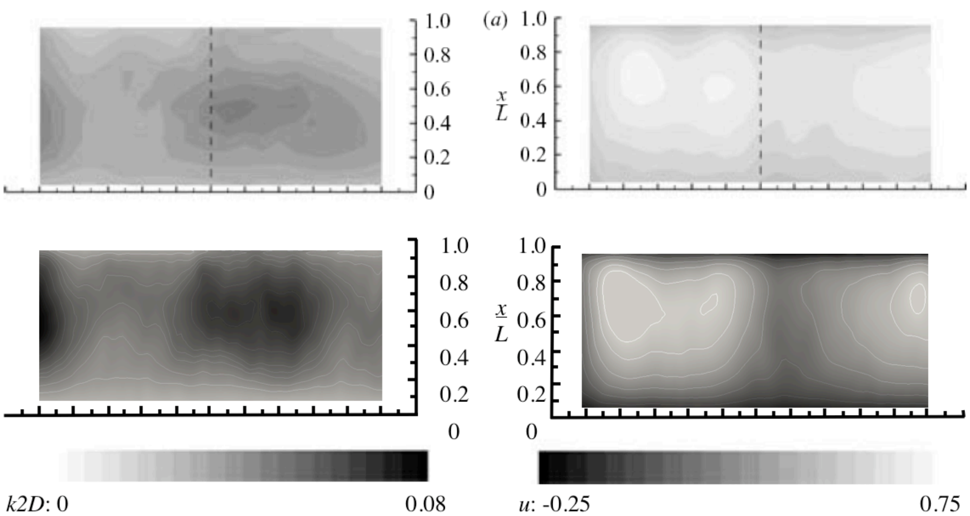

Figure 8: Maps in the horizontal aperture plane of the cavity. Top: measurements of Forestier *et al.* [7] Bottom: LES with the Localized Dynamic Smagorinsky Model for the subsonic cavity. Left: Streamwise velocity. Right: two-dimensional turbulent kinetic energy.

The asymmetric character of the experimental flowfield is also captured, as it is seen from the maps of the streamwise velocity and of the 2D turbulent kinetic energy in the horizontal aperture plane of the cavity (Fig. 8). This bifurcation of the flowfield is induced by the confinement within the lateral walls as demonstrated by Larchevêque *et al.* [12]

5 COMPARISON BETWEEN IMMERSED BOUNDARY METHOD AND CHARACTERISTIC BOUNDARY CONDITIONS

The difference between the characteristic boundary conditions and the Neumann combined to a Dirichlet like conditions for the wall has been first studied by Lamarque *et al.*[34] The possible impact of an IBM reconstruction compared to a classical wall treatment with a wall coinciding exactly with the grid mesh needs also to be assessed. The behavior and accuracy of the immersed boundary method with Neumann and Dirichlet like conditions versus a characteristic formulation has then be investigated.

The first case is a tridimensional flow configuration where a spherical pressure wave develops freely within a closed box of side $L = 0.013m$. The pressure field is initialized with a Gaussian-shaped pressure pulse given by:

$$p(r) = p_\infty \Big[1 + \delta exp \Big(- \frac{r^2}{2R_p^2} \Big) \Big] \quad (1)$$

where $r = \sqrt{x_1^2 + x_2^2 + x_3^3}$ is the distance from the center of the computational domain, R_p is the characteristic dimension of the pressure pulse ($R_p = 0.05L$), δ is the amplitude of the Gaussian-shape pressure pulse ($\delta = 0.001$), T_0=300 K and p_∞=1 atm are the initial parameters.

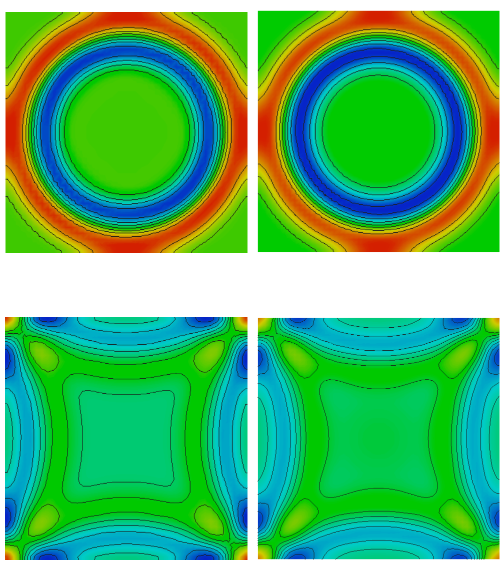

Figure 9: Pressure map and pressure contours at two different times. Immersed boundary method (left) and 3D-NSCBC wall formulation (right).

The present computations have been done with a conforming grid with 3D-NSCBC formalism and with a non-conformal grid with a immersed boundary method. The Fig. 9 shows the pressure field and the pressure contours over a cutting plane at two different times. The two approaches preserve pressure wave front curvature and similar pressure maps.

To estimate the accuracy of the immersed boundary method, the simulations performed previously with non conforming grid meshes are then reiterated with conforming 3D-NSCBC conditions treatment for the cavity walls. The aim of this study is to show that the small discrepancies observed between experimental and numerical ones are not caused by the boundary conditions (Neumann and Dirichlet like conditions with interpolation to rebuild the real border). Since the aeroacoustic loop is generated by the reflection of waves on the downstream wall, spurious reflection as well as bad reflections properties could alter the coupling.

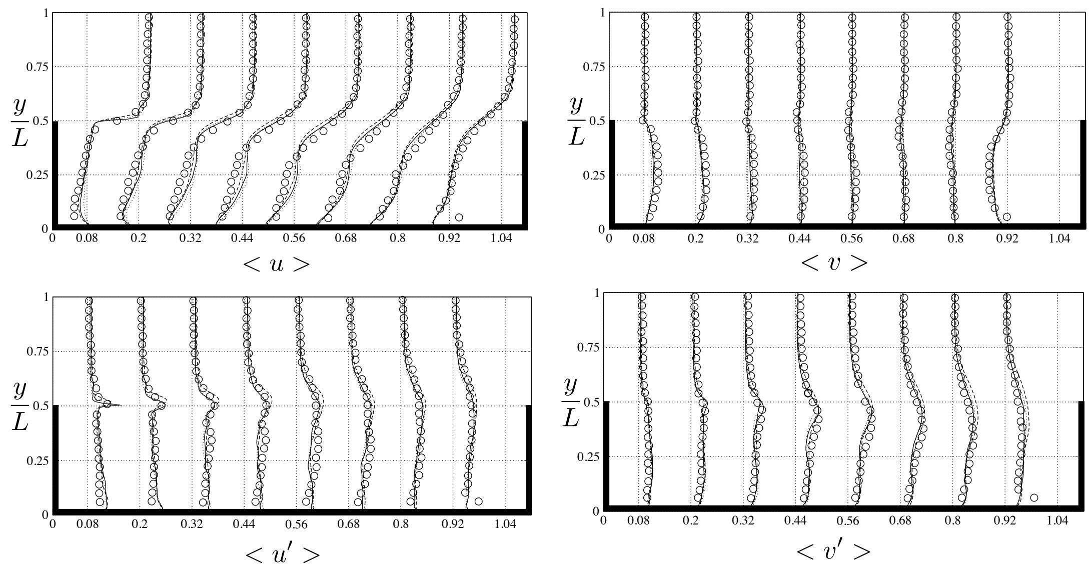

Figure 10: Velocity statistics in the mid-span plane with 3D-NSCBC and conforming multi-grid: longitudinal mean velocity, vertical mean velocity, longitudinal fluctuating velocity and vertical fluctuating velocity: — LDSM, - - - MiLES, · · · Vreman model and ∘ experimental data.

The Fig. 10 shows the statistical features of the cavity flow with the multi-block approach combined with 3D-NSCBC boundary treatment keeping the grid resolution of the previous section. The statistics are identical to the last ones obtained in the IBM framework.The two boundary treatments are found to have no impact on the statistics. No discrepancies seem to be induced by the interpolations on the compressible pattern. Both Neumann and Dirichlet like conditions preserves then the reflective characteristics of the walls.

6 CONCLUSIONS

The Immersed Boundary Method appears as a valuable tool for addressing highly compressible flow fields. The essential features of a transonic cavity flow are recovered by IBM. Quantitative and qualitative agreement with experimental data have been obtained with the immersed boundary concept and with various SGS description for the Large Eddy Simulations. This demonstrates the strong potential of LES-IBM to simulate compressible flow and its ability to describe the feedback process which is based on the interaction of small instabilities in the shear layer with the downstream corner and the generation of acoustic waves which propagate upstream.

Future work will focus on a coupling strategy between immersed boundary methods and combustion modeling and on the description of the trapped vortex complex mechanisms depending on various parameters (structural and aerodynamic).

7 ACKNOWLEDGMENTS

The investigations presented in this paper have been done as a part of the European research project TECC-AE - FP7 (Technologies Enhancement for Clean Combustion in Aero-Engines), Grant No. 2010-020152. Computing resources were provided by GENCI, IDRIS-CNRS and CRIHAN. Dr. L. Larchevêque is gratefully acknowledged for fruitful discussions.

REFERENCES

[1] C. L. Oberg, Combustion stabilization with acoustic cavities (acoustic cavity resonators use for suppression of combustion instability modes, determining acoustic impedance and damping), *J. Spacecraft and Rockets*, **Vol. 8**, 1220-1225 (1971).

[2] K. Hsu and W. M Roquemore, Characteristics of a trapped vortex combustor, *J. Propulsion and Power*, **Vol.14** (1) (1998).

[3] V. Katta and W. M. Roquemore, Numerical studies on trapped-vortex concepts for stable combustion, *Transactions of the ASME*, 120 (1998).

[4] C. Bruno and M. Losurdo, The Trapped Vortex Combustor : An advanced combustion technology for Aerospace and Gas Turbine Applications, in Advanced Combustion and Aerothermal Technologies, 365-384, *NATO Science for Peace and Security Series C: Environmental Security*, Number 6 (2007).

[5] C. S. Peskin, Flow patterns around heart valves : a numerical method, *J. Comput. Phys.*, **Vol.10**, 252-271 (1972).

[6] N. Forestier, Etude expérimentale dune couche cisaillée au-dessus dúne cavité en régime transsonique, PhD thesis, Ecole Centrale de Lyon (2003).

[7] N. Forestier, P. Geffroy and L. Jacquin, Etude expérimentale des propriétés instationnaires dune couche de mélange compressible sur une cavité: cas dune cavité ouverte peu profonde. Rt 22/00153 dafe, ONERA (in French) (2003).

[8] X. Gloerfelt , Bruit rayonné par un écoulement affleurant une cavité: Simulation aéroacoustique directe et application de méthodes intégrales. PhD thesis, Ecole Centrale de Lyon (2001).

[9] Y. Dubief and F. Delcayre, On the coherent-vortex identification in turbulence, *J. Turbulence*, **Vol. 1** (1), 11 (2000).

[10] L. Larchevêque, P. Sagaut, I. Mary and O. Labbé, Large-eddy simulation of a compressible flow past a deep cavity, *Phys. Fluids.*, **Vol. 15** (1), 193-210 (2003).

[11] L. Larchevêque, P. Sagaut, T. H. Le and P. Comte, Large eddy simulation of a compressible flow in a three dimensional open cavity at high Reynolds number, *J. Fluid Mech.*, **Vol. 516**, 265-301 (2004).

[12] L. Larchevêque, P. Sagaut and O. Labbé, Large-eddy simulation of a subsonic cavity flow including asymmetric three-dimensional effects, *J. Fluid Mech.*, **Vol. 577**, 105-126 (2007).

[13] P. Sagaut, E. Garnier, E. Tromeur , L. Larchevêque and E. Labourasse, Turbulent inflow conditions for large-eddy simulation of supersonic and subsonic wall flows, *AIAA Journal*, **Vol. 42**, 469-477 (2004).

[14] F. Ducros, F. Laporte, T. Soulères, V. Guinot, P. Moinat and B. Caruelle, High-order fluxes for conservative skew-symmetric-like schemes in stuctures meshes: Application to compressible flows, *J. Comput. Phys.*, **Vol. 161**, 114-139 (2000).

[15] S. Tatsumi, L. Martinelli and A. Jameson, Flux-limited schemes for the compressible Navier- Stokes equations, *AIAA Journal*, **Vol. 33** (2), pp. 252-261 (1995).

[16] S. Gottlieb and C. Shu, Total Variation Diminishing Runge-Kutta schemes, *Mathematics of Computation*, **Vol. 67** (221), 73-85 (1998).

[17] G. Lodato, P. Domingo and L. Vervisch, Three-Dimensional boundary conditions for direct and large eddy simulation of compressible viscous flows, *J. Comput. Phys.*, **Vol. 227** (10), 5105-5143 (2008).

[18] E. Lamballais and J. Silvestrini, Direct numerical simulation of interactions between a mixing layer and a wake around a cylinder, *J. Turbulence.*, **Vol. 3** (2002).

[19] P. De Palma, M.D. de Tullio, G. Pascazio and M. Napolitano, An immersed boundary method for compressible viscous flows, *Comput. Fluids*, Vol. 35, 693 (2006).

[20] E. A. Fadlun, R. Verzicco, P. Orlandi and J. Mohd-Yusof, Combined Immersed-Boundary Finite-Difference Methods for Three-Dimensional Complex Flow Simulations, *J. Comput. Phys.*, **Vol. 161**, 35-60 (2000).

[21] G. Iaccarino and R. Verzicco, Immersed boundary technique for turbulent flow simulations, *Appl. Mech. Rev.*, **Vol. 56** (3), 331-347 (2003).

[22] R. Ghias, R. Mittal and H. Dong, A sharp interface immersed boundary method for compressible viscous flows, *J. Comput. Phys.*, **Vol. 225**, 528-553 (2007).

[23] E. Balaras, Modeling complex boundaries using an external force field on fixed Cartesian grids in large eddy simulations, *Computers and Fluids*, **Vol. 33** (3), 375-404 (2004).

[24] F. F. Grinstein and C. Fureby, Recent progress on Miles for high Reynolds number flows, *J. Fluids Eng.*, **Vol. 24**, 848-861 (2002).

[25] A. W. Vreman, An eddy-viscosity subgrid-scale model for turbulent shear flow: Algebraic theory and applications, *Phys. Fluids.*, **Vol. 16** (10) (2004).

[26] C. Meneveau, T. Lund and W. Cabot, A lagrangian dynamic subgrid-scale model of turbulence, *J. Fluid Mech.*, **Vol. 319**, 353-385 (1996).

[27] S. Ghosal, T.S. Lund, P. Moin and K. Akselvoll, A dynamic localization model for large eddy simulation of turbulent flows, *J. Fluid Mech.*, **Vol. 286**, 229-255 (1995).

[28] Y. Zang, R. L. Street and J. R. Koseff, A dynamic mixed subgrid-scale model and its application to turbulent recirculating flows, *Phys. Fluids.* A, **Vol. 5** (12), 3186-3196 (1993).

[29] T. Ye, R. Mittal, H. S. Udaykumar and W. Shyy, An accurate cartesian grid method for viscous incompressible flows with complex immersed boundaries, *J. Comput. Phys.*, **Vol. 156**, 209-240 (1999).

[30] C. H. K. Williamson. Vortex dynamics in the cylinder wake, *Ann. Rev. Fluid. Mech.*, **Vol. 28**, 2477-539 (1996).

[31] D. A. Lyn, S. Einavv, W. Rodi and J. H. Park, A Laser-Doppler Velocimetry study of ensemble-averaged characteristics of the turbulent near wake of a square cylinder, *J. Fluid Mech.*, **Vol. 304**, 285-319 (1995).

[32] I. McLean and I. Gartshore, Spanwise correlation of pressure on a rigid square section cylinder, *J. Wind Engineering*, **Vol. 41**, 779-808 (1992).

[33] M. Klein, A. Sadiki and J. Janicka, A digital filter based genration of inflow data for spatially developing direct numerical or large eddy simulation, *J. Comput. Phys.*, **Vol. 186**, 652-665 (2003).

[34] N. Lamarque, M. Porta, F. Nicoud and T. Poinsot, On the stability and dissipation of wall boundary conditions for compressible flows, *Int. J. Numer. Meth. Fluids*, **Vol. 62**, 1134-1154 (2010).